

## Modeling solute transport in poroelastic shale

I.Q. Khaydarov

**Abstract.** The paper is devoted to modeling the solvent and solute transfer in a chemically inert elastically deformable rock, the model takes into account only the variation in stress and pore pressure. Chemical effects are taken into account by changing the pore pressure and deformation of rocks in the transport equations. For the numerical solution of the problem, combinations of the Laguerre integral transformation method and the finite difference method are used. The results of simulation for the model of solute transport through semipermeable shale are presented.

### Introduction

The presence of pore fluids can affect the deformation process and facilitate or delay the destruction of the material [1]. Rock expansion while undrained deformation causes a decrease in pore pressure and an increase in the limiting stress value [2]. On the other hand, the response causes an increase in pore pressure and a decrease in fracture stress [3].

An important stability mechanism for wells drilled in reactive shale formations with water-based drilling fluids is based on the physicochemical interactions between rock and drilling fluid. Namely, the pore pressure in the bottomhole zone can be reduced due to the osmotic outflow of the pore fluid from the reactive shale, which is caused by increased mineralization of the drilling fluid [4–7].

The theory developed in [8, 9] to describe coupled mechanical, hydraulic, and chemical interactions for liquid-filled porous bodies is based on a modification of Biot's theory of poroelasticity [10–12].

In applied problems of elastic wave propagation, there is often a need to take into account the porosity, fluid saturation of the medium, and the hydrodynamic background. In particular, these aspects arise in exploration geophysics when searching for oil layers and when choosing the parameters of wavy impact on oil and gas fields for stimulating the production. Similar issues exist in seismology in the geophysical monitoring of the properties of the source zone in order to predict earthquakes [13]. Real media are porous, fractured and energy-absorbing (energy is lost in the system).

Following [9], for simplicity, we consider a porous liquid consisting of one uncharged solute with a mole fraction  $\Psi = x^s$  in a solvent (water) with a molar fraction  $x^w = 1 - \Psi$ . The solution is considered ideal. The chemical potentials of a solute  $\mu^s$  and a solvent  $\mu^w$  have the form

$$\mu^s = pV_s + RT \ln \Psi, \quad \mu^w = pV_w + RT \ln(1 - \Psi).$$

The molar volume of a solution (at atmospheric pressure) is

$$V_{\text{sol}} = (1 - \Psi)V_w + \Psi V_s.$$

In [14], a chemoporoelastic model was considered for estimating the stress profile of the near-wellbore space, and in [15], a system of chemo-thermo-poroelasticity equations was solved using the implicit finite-difference method. Further, in the presented paper, we assume (as in [9]) that the bulk modulus  $K$  of the solution is independent of  $\Psi$ , and the problem is restricted to the isothermal case at a constant temperature.

### 1. Statement of the problem of solute transport in poroelastic shale

Using the laws of conservation of mass and assuming that  $\Psi$  exhibits a weak change [9], and after simple transformations, we obtain a system of parabolic equations:

$$\frac{\partial \Phi}{\partial t} = A \nabla^2 \Phi + H \nabla^2 \Psi, \quad (1)$$

$$\frac{\partial \Psi}{\partial t} = C \nabla^2 \Phi + E \nabla^2 \Psi, \quad (2)$$

where  $\Phi = \sigma_{kk} + \frac{3p}{B}$ ,  $\sigma_{kk}$  is the trace of the stress tensor,

$$A = \frac{2GB^2k(1-\nu)(1+\nu_u)^2}{9(1-\nu_u)(\nu_u-\nu)V_{\text{sol}}} [\gamma V_s x_0^s + V_w(1-x_0^s)],$$

$$H = \frac{2GB(1+\nu)(1+\nu_u)(\gamma-1)RTk}{3(\nu_u-\nu)},$$

$$C = \frac{(\gamma-1)Bk(1-\nu)(1+\nu_u)V_s V_w x_0^s (1-x_0^s)}{3(1-\nu_u)(1+\nu)\alpha V_{\text{sol}}},$$

$$E = \frac{V_s}{\alpha V_{\text{sol}}} [\gamma D V_{\text{sol}} + (1-\gamma)RTk x_0^s],$$

$\gamma$  is the transmittance, and  $D$  is the diffusion coefficient.

The functions  $\Phi(x, t)$  and  $\Psi(x, t)$  in the one-dimensional case are determined from the system of heat conduction equations

$$\frac{\partial \Phi}{\partial t} = A \frac{\partial^2 \Phi}{\partial x^2} + H \frac{\partial^2 \Psi}{\partial x^2}, \quad 0 < x < L, \quad t > 0, \quad (3)$$

$$\frac{\partial \Psi}{\partial t} = C \frac{\partial^2 \Phi}{\partial x^2} + E \frac{\partial^2 \Psi}{\partial x^2}, \quad 0 < x < L, \quad t > 0, \quad (4)$$

with boundary conditions

$$\Phi|_{x=0} = \Phi_0(t), \quad \Phi|_{x=L} = \Phi_1(t), \quad t > 0, \quad (5)$$

$$\Psi|_{x=0} = \Psi_0(t), \quad \Psi|_{x=L} = \Psi_1(t), \quad t > 0, \quad (6)$$

and zero Cauchy data

$$\Phi|_{t=0} = 0, \quad \Psi|_{t=0} = 0, \quad 0 < x < L. \quad (7)$$

To solve the initial-boundary value problem (3)–(7), we use the Laguerre method of integral transformation in time [16–18].

After applying the Laguerre transform, the original problem (3)–(7) is reduced to a one-dimensional boundary value problem for an ordinary differential system in the spectral region, which is rewritten as:

$$\frac{h}{2}\Phi^m = A\frac{d^2\Phi^m}{dx^2} + H\frac{d^2\Psi^m}{dx^2} - h\sum_{k=0}^{m-1}\Phi^k, \quad 0 < x < L, \quad (8)$$

$$\frac{h}{2}\Psi^m = C\frac{d^2\Phi^m}{dx^2} + E\frac{d^2\Psi^m}{dx^2} - h\sum_{k=0}^{m-1}\Psi^k, \quad 0 < x < L \quad (9)$$

with boundary conditions

$$\Phi^m|_{x=0} = \Phi_0^m, \quad \Phi^m|_{x=L} = \Phi_1^m, \quad (10)$$

$$\Psi^m|_{x=0} = \Psi_0^m, \quad \Psi^m|_{x=L} = \Psi_1^m. \quad (11)$$

To solve problem (8)–(11), we use a finite-difference method with the second order of accuracy [18].

## 2. Numerical results

For numerical calculations, a hyperbolic system with the corresponding initial-boundary conditions (5)–(7) was considered instead of the parabolic system (3), (4). Figures 1–4 show the results of seismic traces for  $\Phi(t)$  and  $\Psi(t)$  components calculated for a two-layer medium.

For our calculations, two different two-layer models of the medium with the following common physical characteristics were set:  $x_0^s = 0.1$ ,  $\varphi = 0.14$ ,  $B = 0.92$ ,  $T = 300$  K,  $\nu = 0$ ,  $\nu_u = 0.44$ ,  $V_w = 1.8 \cdot 10^{-5}$  m<sup>3</sup>,  $V_s = 2.6 \cdot 10^{-5}$  m<sup>3</sup>,  $R = 8.3$  J K<sup>-1</sup> Mol<sup>-1</sup>.

The boundaries of the first layer were defined as  $0 \leq x \leq 5 \cdot 10^{-4}$ , and for the second layer this was  $5 \cdot 10^{-4} \leq x \leq 10^{-3}$ .

The wave field was modeled from a source located at the left end of the first poroelastic layer:  $\Phi_0(t) = 0$ ,  $\Phi_1(t) = 0$ ,  $\Psi_0(t) = f(t)$ ,  $\Psi_1(t) = 0$ . The time signal in the source was given in the form

$$f(t) = \exp\left(-\frac{2\pi f_0(t-t_0)^2}{\kappa^2}\right) \sin(2\pi f_0(t-t_0)),$$

where  $\kappa = 4$ ,  $f_0 = 1$  Hz,  $t_0 = 1.5$  s.

For the calculations presented in Figures 1–2, the following characteristics of both layers were specified: diffusion coefficient  $D = 10^{-7}$  m<sup>2</sup>/s and permeability  $k = 1.4 \cdot 10^{-20}$  m<sup>2</sup>. For the first layer we assign the shear modulus  $G = 0.6$  GPa and transmittance  $\gamma = 0.7$ . For the second layer we assign the shear modulus  $G = 1$  GPa and the transmittance  $\gamma = 0.2$ .

Therefore, the coefficients of system (7), (8) for the first layer are defined as  $A = 0.280 \cdot 10^{-10}$ ,  $H = -0.899 \cdot 10^{-8}$ ,  $C = -0.286 \cdot 10^{-25}$ ,  $E = 0.126 \cdot 10^{-10}$ , and hence the velocities of elastic vibrations in this layer are the following:  $A_1 = 0.530 \cdot 10^{-5}$  m/s,  $A_2 = 0.355 \cdot 10^{-5}$  m/s.

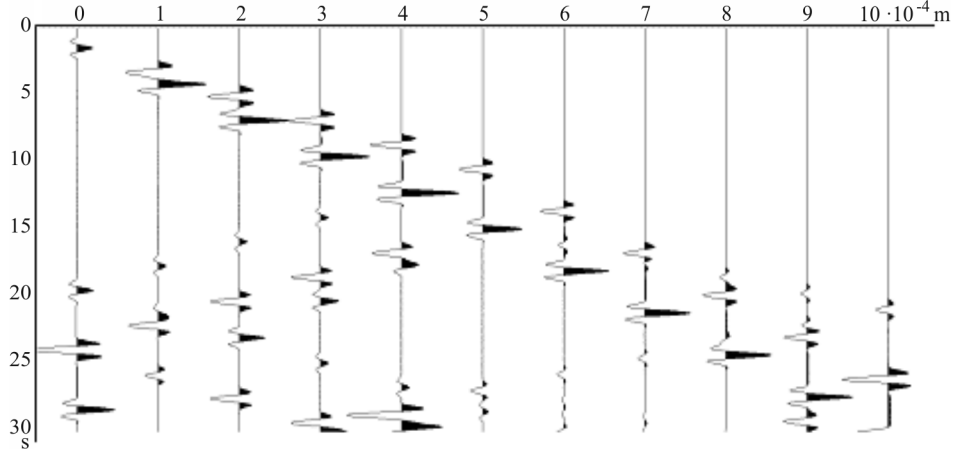


**Figure 1.** Traces for the component  $\Phi(t)$

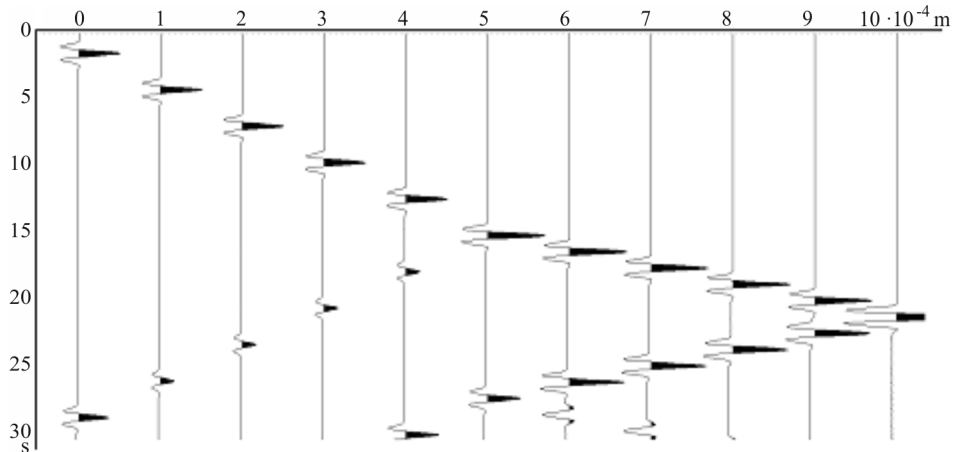


**Figure 2.** Traces for the component  $\Psi(t)$

The system coefficients for the second layer are defined as  $A = 0.936 \cdot 10^{-11}$ ,  $H = -0.299 \cdot 10^{-8}$ ,  $C = -0.285 \cdot 10^{-25}$ ,  $E = 0.631 \cdot 10^{-10}$ , and hence the velocities of elastic vibrations in this layer  $A_1 = 0.794 \cdot 10^{-5}$  m/s,  $A_2 = 0.306 \cdot 10^{-5}$  m/s.

For the calculations presented in Figures 3 and 4, the second model was set with the general characteristics of both layers — the permeability  $k = 2 \cdot 10^{-20}$  m<sup>2</sup>. For the first layer we take the diffusion coefficient  $D = 10^{-7}$  m<sup>2</sup>/s, shear modulus  $G = 0.6$  GPa and transmittance  $\gamma = 0.7$ . For the second layer the values are following: diffusion coefficient  $D = 2 \cdot 10^{-6}$  m<sup>2</sup>/s, shear modulus  $G = 1$  GPa and transmittance  $\gamma = 0.2$ .

Therefore, the coefficients of system (7), (8) for the first layer are defined as  $A = 0.182 \cdot 10^{-10}$ ,  $H = -0.180 \cdot 10^{-7}$ ,  $C = -0.572 \cdot 10^{-25}$ ,  $E = 0.982 \cdot$

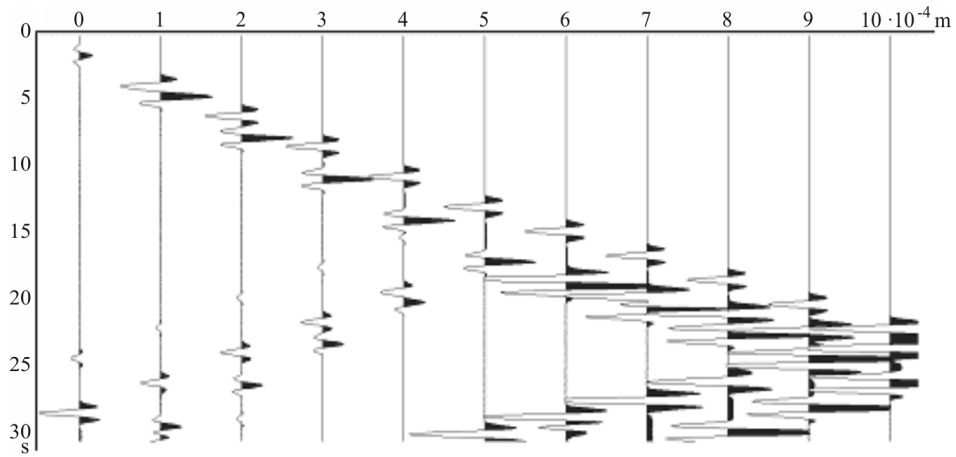


**Figure 3.** Traces for the component  $\Phi(t)$

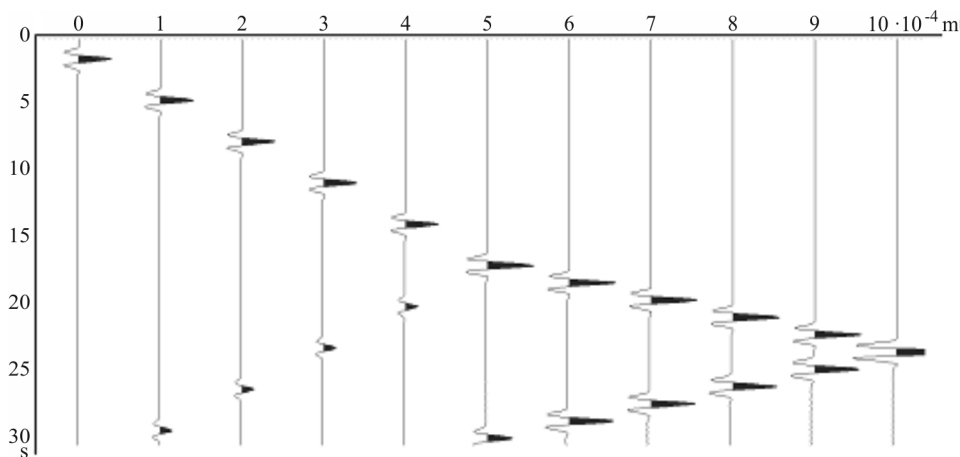


**Figure 4.** Traces for the component  $\Psi(t)$

$10^{-11}$ , and hence the velocities of elastic vibrations in this layer  $A_1 = 0.427 \cdot 10^{-5}$  m/s,  $A_2 = 0.313 \cdot 10^{-5}$  m/s.

The system coefficients for the second layer are defined as  $A = 0.282 \cdot 10^{-10}$ ,  $H = -0.8 \cdot 10^{-7}$ ,  $C = -0.152 \cdot 10^{-24}$ ,  $E = 0.561 \cdot 10^{-10}$ . Hence, the velocities of elastic vibrations in this layer are estimated as  $A_1 = 0.749 \cdot 10^{-5}$  m/s,  $A_2 = 0.531 \cdot 10^{-5}$  m/s.

It can be seen from the presented figures, the corresponding two types ( $A_1$  and  $A_2$ ) of transmitted and reflected waves for the component  $\Phi(x, t)$  were generated. The wave  $A_2$ -type for the component  $\Psi(x, t)$  was generated.

Figures 5 and 6 show the results of calculations for the parabolic system (3), (4) with the initial-boundary conditions (5)–(7). Calculations for the second version of two-layer medium are presented.

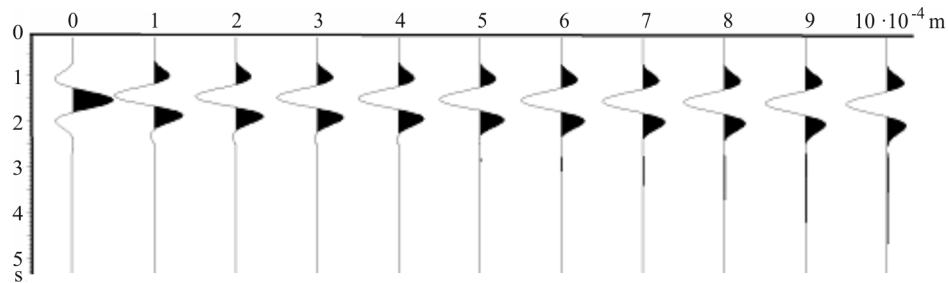


**Figure 5.** Traces for the component  $\Phi(t)$ . The normalization is independent for each trace

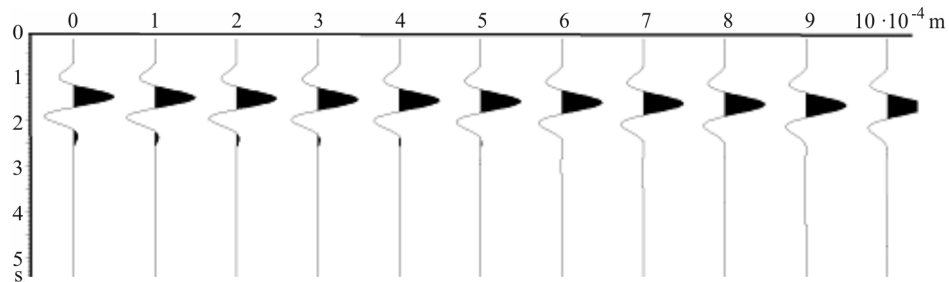


**Figure 6.** Traces for the component  $\Psi(t)$ . The normalization is independent for each trace

## References

- [1] Mroz Z., Boukpeti N., Drescher A. Constitutive model for static liquefaction // Int. J. Geomech. ASCE. — 2003. — No. 3. — P. 133–144.
- [2] Rice J.R. On the stability of dilatant hardening for saturated rock masses // J. Geophys. Res. — 1975. — Vol. 80, No. 11. — P. 1531–1536.

- 
- [3] Boukpeti N., Mroz Z., Drescher A. A model for static liquefaction in triaxial compression and extension // *Can. Geotech. J.* — 2002. — Vol. 39. — P. 1243–1253.
- [4] van Oort E., Hale A.H., Mody F.K., Roy S. Transport in shales and the design of improved water-based shale drilling fluids // *SPE Drilling & Completion.* — 1996. — P. 137–146 (paper #28309).
- [5] Nguyen V., Abousleiman Y., Hoang S. Analysis of wellbore instability in drilling through chemically active fractured rock formations // *SPE J.* — 2009. — Vol. 14, No. 2. — P. 283–301.
- [6] Ghassemi A., Tao Q., Diek A. Influence of coupled chemo-poro-thermoelastic processes on pore pressure and stress distributions around a wellbore in swelling shale // *J. Petroleum Science and Engineering.* — 2009. — Vol. 67, No. 1–2. — P. 57–64.
- [7] Zhou X., Ghassemi A. Finite element analysis of coupled chemo-poro-thermo-mechanical effects around a wellbore in swelling shale // *Intern. J. Rock Mechanics and Mining Sciences.* — 2009. — Vol. 46, No. 4. — P. 769–778.
- [8] Sherwood J.D. Biot poroelasticity of a chemically active shale // *Proc. Roy. Soc. — London*, 1993. — Vol. 440. — P. 365–377.
- [9] Sherwood J.D. A model of hindered solute transport in a poroelastic shale // *Proc. Roy. Soc. — London*, 1994. — Vol. 445. — P. 679–692.
- [10] Biot M.A. General theory of three-dimensional consolidation // *J. Appl. Phys.* — 1941. — Vol. 12. — P. 155–164.
- [11] Detournay E., Cheng A.H-D. *Comprehensive Rock Engineering*, Vol. 2, Ch. 5: Fundamentals of Poroelasticity. — New York: Pergamon, 1993. — P. 113–171.
- [12] Coussy O. *Poromechanics.* — New York: Wiley, 2004.
- [13] Alekseev A.S., Imomnazarov Kh.Kh., Grachev E.V., et al. Direct and inverse dynamic problems for the system of equations of the continuum theory of filtration // *Siberian J. Industrial Mathematics.* — 2004. — Vol. 7, No. 1. — P. 3–8 (In Russian).
- [14] Roshan H., Rahman S. A fully coupled chemo-poroelastic analysis of pore pressure and stress distribution around a wellbore in water active rocks // *Rock Mechanics and Rock Engineering.* — 2011. — Vol. 44. — P. 199–210.
- [15] Rafieepour S., Zamiran S., Ostadhassan M. A cost-effective chemo-thermo-poroelastic wellbore stability model for mud weight design during drilling through shale formations // *J. Rock Mechanics and Geotechnical Engineering.* — 2020. — No. 12. — P. 768–779.
- [16] Mikhailenko B.G., Mikhailov A.A., Reshetova G.V. Numerical modeling of transient seismic fields in viscoelastic media based on the Laguerre spectral method // *Pure Appl. Geophys.* — 2003. — Vol. 160. — P. 1207–1224.

- [17] Mikhailenko B.G., Mikhailov A.A., Reshetova G.V. Numerical viscoelastic modeling by the spectral Laguerre method // *Geophysical Prospecting*. — 2003. — Vol. 51. — P. 37–48.
- [18] Imomnazarov B.Kh., Mikhailov A.A., Khaidarov I.K., Kholmuradov A.E. Numerical solution of the problem of solute transport in poroelastic shale // *Siberian Electron. Math. Izvestiya* — 2021. — Vol. 18, No. 1. — P. 694–702 (In Russian).